Proc. Natl. Acad. Sci. USA
Vol. 93, pp. 5460–5465, May 1996
Applied Biological Sciences

Irreversible inactivation of interleukin 2 in a pump-based delivery environment

(interleukin 2 physical stability/protein delivery/protein–surface interactions)

STELIOS T. TZANNIS*, WILLIAM J. M. HRUSHESKY†, PATRICIA A. WOOD†, AND TODD M. PRZYBYCIEN*‡

*The Howard P. Isermann Department of Chemical Engineering, Applied Protein Biophysics Laboratory, Rensselaer Polytechnic Institute, Troy, NY 12180-3590; and †Department of Medical Oncology, Stratton Veterans Adminstration Medical Center, Albany, NY 12208

Communicated by Robert Langer, Massachusetts Institute of Technology, Cambridge, MA, October 23, 1995

ABSTRACT **The physical stability of pharmaceutical proteins in delivery environments is a critical determinant of biological potency and treatment efficacy, and yet it is often taken for granted. We studied both the bioactivity and physical stability of interleukin 2 upon delivery via continuous infusion. We found that the biological activity of the delivered protein was dramatically reduced by ≈90% after a 24-hr infusion program. Only a portion of these losses could be attributed to direct protein deposition on the delivery surfaces. Analysis of delivered protein by size exclusion chromatography gave no indication of insulin-like, surface-induced aggregation phenomena. Examination of the secondary and tertiary structure of both adsorbed and delivered protein via Fourier-transform infrared spectroscopy, circular dichroism, and fluorescence spectroscopy indicated that transient surface association of interleukin 2 with the catheter tubing resulted in profound, irreversible structural changes that were responsible for the majority of the biological activity losses.**

The physical stability of formulated therapeutic proteins in delivery environments is a necessity for successful short- or long-term delivery via implantable or portable pumps. Protein delivery device surface interactions may induce conformational changes and aggregation, which may result in the inactivation of the delivered protein and therefore compromise the intended therapeutic benefit.

Protein–surface interaction phenomena have been studied extensively over the past 15 years. However, the focus has typically been to assess implantable materials for hemocompatibility (1). A notable exception is given by the extensive studies of the delivery of insulin via micropumps, which have shown surface-induced aggregation and consequent inactivation phenomena (2, 3). It has also been demonstrated that administration of low concentrations of interleukin (IL)-1β via a syringe–pump system results in adsorptive losses of 20–80% (4). Our previous studies revealed ≈99% losses in the biological activity of formulated IL-2 after 24-hr exposure to commercial silicone rubber tubing in a recirculating system (S.T.T., J. M. Hrushesky, P.A.W., & T.M.P., unpublished work). Similarly, reductions of 80–90% of the biological activity of a Food and Drug Administration-approved IL-2 formulation have been reported during delivery via polyethylene catheter tubing (6). Addition of human serum albumin or surfactants to the reconstitution medium can significantly decrease adsorptive losses (2, 4, 7), although in the case of IL-2, the effectiveness of human serum albumin as a passivating agent is limited (6).

In the present effort, we assessed the nature and extent of interactions of a commercial IL-2 formulation with a portable infusion pump/catheter tubing system. We also explored the impact of these interactions on the active delivery profile and established a structure–function relationship for both the adsorbed and delivered protein via a variety of spectroscopic techniques. IL-2 is a potent anti-tumor and immune modulator that has been administered using both high-dose bolus and continuous infusion strategies with promising clinical results in the treatment of cancer and acquired immune deficiency syndrome (AIDS). Moreover, IL-2 is representative of the hematopoietic growth factor family, with high sequence and structural homology with other therapeutic proteins such as granulocyte colony-stimulating factor, granulocyte macrophage colony-stimulating factor, erythropoietin, and growth hormone. The IL-2 case may serve as a paradigm for the optimal delivery of these therapeutic proteins.

MATERIALS AND METHODS

Materials. Recombinant human interleukin-2 (IL-2) expressed in *E. coli* (RU 49637, Batch no. BV 23621-066A; Roussel-Uclaf) was obtained as a monomeric, powdered clinical formulation ($1.2 \pm 0.6 \times 10^7$ units/mg) with 0.01 mg of isopropanol per 0.5 mg of IL-2. The powder was stored at −20°C before use and was reconstituted in 10 mM phosphate buffer (pH 7.4) with 150 mM NaCl at 25°C. The delivery system consisted of a programmable, portable, piston-operated clinical infusion system (Panomat V-5; Disetronic Medical Systems, Plymouth MN) connected to a 60-cm length of 1.0-mm i.d. radiopaque medical grade silicone rubber catheter tubing (Dow-Corning) provided by Medtronic (Minneapolis). The tubing was cleaned, steam-sterilized, and hydrated with water for injection-grade water before use.

Delivery Apparatus and Protocol. The borosilicate glass reservoir of the pump was loaded under sterile conditions with freshly reconstituted IL-2 solution at a concentration of either 0.1 or 0.05 mg per ml and then connected to the catheter tubing. The entire experimental system was placed in a 37°C incubator. Following actual clinical protocols, the tubing was primed with the protein solution at the initiation of the experiment. The solution was pumped at 100 μL per hr and collected in 300-μl capacity sterile vials (flow system). Under these conditions the Reynolds number was 0.05, the wall shear rate was 0.28 sec^{-1}, and the Peclet number was 0.5. At 2, 6, and 24 hr, a 10-cm portion of the tubing was removed from the collection vial end of the system and subjected to Fourier-transform infrared (FTIR) analysis. In order to control for exposure at 37°C and adsorption on the pump reservoir walls, a similar reservoir loaded with IL-2 solution of the same volume and concentration was placed in the incubator (non-flow system) and similarly sampled over 24 hr.

Delivered Protein Characterization. *Bioactivity.* IL-2 biological activity was assessed via a proliferation assay based on the IL-2-dependent mouse spleen cell line, CTLL-2; this assay is described in detail elsewhere (Tzannis *et al.*, unpublished work).

The publication costs of this article were defrayed in part by page charge payment. This article must therefore be hereby marked "*advertisement*" in accordance with 18 U.S.C. §1734 solely to indicate this fact.

Abbreviations: IL, interleukin; FTIR, Fourier-transformed infrared.

‡To whom reprint requests should be addressed.

Downloaded at Palestinian Territory, occupied on December 20, 2021

Protein concentration. The bicinchoninic acid protein determination method (Pierce) was used to quantitate the concentration of delivered IL-2 over time.

Secondary structure. Solution phase IL-2 secondary structure was characterized via far-UV CD, using a previously reported spectral acquisition and manipulation protocol (8) in conjunction with the structure fitting technique of Sreerama and Woody (9).

Tertiary structure. Fluorescence spectroscopy was used to examine the environment of Trp^{121}, the lone tryptophan of IL-2. Steady-state fluorescence measurements were performed on a Perkin–Elmer LS50B Luminescence spectrophotometer equipped with a Neslab RTE-111 thermostat (Neslab Instruments, Portsmouth, NH) set at 25°C. The samples were excited at 295 nm (10), and five emission spectra, recorded between 300–450 nm with a 1-nm band width, were collected and averaged; the excitation and emission slits were set at 4.5 nm. We also used iodide and acrylamide in static quenching experiments to probe the solvent accessibility of Trp^{121} (10–12). Iodide was added from a 5 M stock solution in the reconstitution buffer along with 1 mM $Na_2S_2O_3$ to prevent I_2 formation, which could cause precipitation of the protein (13). Similarly, acrylamide was added from a 5 M stock solution also in the reconstitution buffer. The emission spectra of the protein solutions were corrected for background scatter, dilution and, in the quenching experiments, absorbance by KI and acrylamide (13, 14).

Aggregation state. The extent of aggregation was determined via size exclusion HPLC analysis as follows: the stationary phase was a 30 cm × 7.8 mm i.d. Ultrahydrogel-250 (Waters) column; the mobile phase consisted of the IL-2 reconstitution buffer; the sample size was 50 μl; the mobile phase flow rate was 0.75 ml/min; and detection was performed at 280 nm by a Waters 486 UV/VIS detector. Relative IL-2 concentrations were determined by peak area integration using the Waters MILLENIUM software package.

Adsorbed Protein Characterization. Attenuated total reflectance FTIR spectroscopy was used to characterize the adsorbed IL-2. Spectra were collected on a Perkin–Elmer 1800 FT-IR spectrophotometer equipped with a DTGS detector that was continuously purged with dry nitrogen. Five hundred twelve double-sided interferograms were collected using a 45° germanium attenuated total reflectance crystal in the 4000–700 cm^{-1} range at 2 cm^{-1} resolution, coadded, triangularly apodized, and Fourier-transformed. IL-2 solution spectra were recorded at 0.1 mg/ml in 10 mM phosphate buffer saline (pH 7.4). The observed spectra consist of contributions from the silicone rubber tubing, adsorbed protein, adherent residual buffer solution, and residual water vapor in the light path; solution spectra have contributions from buffer and water vapor. These contributions were subtracted based on a protocol detailed elsewhere (Tzannis *et al.*, unpublished work).

Surface concentration. The amide II band (1495–1590 cm^{-1}) was used to determine the adsorbed protein concentration (5). The estimated catheter surface concentration for monolayer coverage of IL-2 is 0.41 $\mu g/cm^2$, assuming an Euclidean surface (Tzannis *et al.*, unpublished work). However, topography information for the inner surface of the catheter tubing used in this work, obtained via scanning electron microscopy in the secondary electron mode, indicated that the actual surface area is 2 to 4 times greater than the Euclidean area.

Secondary structure. The amide I (1600–1700 cm^{-1}) band was used to assess the secondary structure content of adsorbed IL-2 as a function of the duration of surface exposure. The spectral processing and fitting routines and their method validation are described elsewhere (Tzannis *et al.*, unpublished work).

RESULTS

Bioactivity of Delivered IL-2. As the results given in Table 1 indicate, the biological activity of delivered IL-2 is severely reduced; after 24 hr of delivery, the 0.1 and 0.05 mg/ml solutions retain only ≈10% and ≈6% of their original activity, respectively. The activity of the nonflow control samples was essentially constant. The majority of these losses occur within the first 2 hr; thereafter the losses continue but at a diminished rate. The activity profile reflects the solution residence time in the catheter. The 0.05 mg/ml system suffered a greater activity loss on a percentage basis than the 0.10 mg/ml system.

To what may these losses be attributed? The unchanged activity of the control samples allows us to rule out any significant role for the pump reservoir surfaces or mere incubation at 37°C. Exposure to the catheter at 37°C must be responsible. We dismiss denaturation due to flow effects in the tubing *a priori*, as Reynolds numbers in the creeping flow regime put wall shear rates at least three orders of magnitude smaller than the threshold reported for enzyme inactivation in Couette flow (15). Nor do we expect chemical degradation over the 24-hr period to be responsible. The known major degradation products of IL-2, oxidized Met^{104} and Cys^{125}, have been shown to retain full activity (16–18); these residues are not crucial for the biological activity of IL-2. Disulfide scrambling is known to diminish IL-2 bioactivity (19), but at the temperature studied, it appears to be significant only at alkaline pH (20). Thus, we suspect that the catheter surface has mediated the physical inactivation of IL-2 by either direct adsorption, aggregation, or denaturation.

Aggregation Status of Delivered IL-2. As IL-2 aggregates often lack biological activity [refs. 17 and 21; although one commercial IL-2 preparation is formulated as a reversible aggregate (refs. 19 and 22)], we examined delivered IL-2 for evidence of increased levels of aggregates. The results in Table 1 show that the delivered IL-2 is at all times largely monomeric. Both the flow and nonflow samples exhibited similar aggregation patterns over the time examined. At all times the chromatograms are characterized by four distinct peaks with the monomer (15.1 ± 0.4 kDa) forming the predominant species ranging from 73 wt % initially to 93 wt % after 24 hr in the flow system. Two higher molecular weight species, which probably reflect dimers/trimers (35.2 ± 0.5 kDa) and pentamers/hexamers (79.4 ± 1.0 kDa), represent only a small portion of the overall delivered protein and decrease with time. These high molecular weight species likely represent reversible aggregates formed upon reconstitution. Further, these aggregates are likely biologically active, as the initial solution activity is within experimental error of the nominal bioactivity expected upon reconsitution per the manufacturer's product literature. The decline and disappearance of high molecular weight species also suggests that the surface-induced inactivation of IL-2 does not proceed through disulfide reduction, because that would probably lead to enhanced self-association in solution. Based on these findings, we conclude that aggregation phenomena cannot explain the observed biological activity losses.

In the course of this analysis of aggregation state, a low molecular weight species (8.0 ± 0.3 kDa) was detected at low levels throughout the 0.1 mg/ml experiments. This apparent cleavage fragment may account for a small percentage of the observed activity losses for these experiments. It is unlikely that this species is the result of a catheter surface-induced cleavage process, because a similar peak (8.4 ± 0.3 kDa) appears at comparable concentrations in the corresponding nonflow control. No such species was observed in the 0.05 mg/ml experiments; if it is present at all, it may be at levels below the detectable limit.

Delivered IL-2 Concentration Profile. Another possibility is that significant amounts of IL-2 have been physically removed

Downloaded at Palestinian Territory, occupied on December 20, 2021

Table 1. Delivered and adsorbed IL-2 assay results

	Surface exposure, 0.1 mg/ml IL-2 solution				Surface exposure, 0.05 mg/ml IL-2 solution			
	Initial solution	2 hr	10 hr	24 hr	Initial solution	2 hr	10 hr	21 hr
			Delivered IL-2					
Bioactivity ($\times 10^5$ units/ml)*								
Flow	3.2 ± 1.2	0.75 ± 0.16	0.52 ± 0.03	0.30 ± 0.09	5.2 ± 1.5	0.53 ± 0.21	0.52 ± 0.22	0.35 ± 0.09
Nonflow	6.8 ± 2.2	ND	ND	6.1 ± 1.9	5.2 ± 1.5	ND	ND	5.35 ± 0.49
Concentration (μg/ml)								
Flow	103 ± 8	77 ± 5‡	79 ± 6	82 ± 7	54 ± 4	34 ± 2‡	34 ± 2	39 ± 3
Nonflow	108 ± 8	106 ± 8‡	106 ± 8	100 ± 7	57 ± 4	55 ± 4‡	55 ± 4	59 ± 4
Mass delivered (% of initial)†	100.0	78.4 ± 6.6‡	77.8 ± 7.2	87.0 ± 9.2	100.0	69.1 ± 7.2‡	68.8 ± 6.6	69.1 ± 5.3
Size distribution (wt %)								
Flow								
Low molecular weight species	0.0	6.1	5.3	4.8	0.0	0.0	0.0	0.0
Monomer	61.9	67.9	92.2	93.0	70.5	61.0	82.2	96.9
Dimer/trimer	27.1	19.1	1.7	0.9	25.1	19.0	10.3	1.1
Pentamer/hexamer	11.0	6.9	0.8	1.3	4.4	20.0	7.5	2.0
Nonflow								
Low molecular weight species	0.0	0.0	11.6	5.0	0.0	0.0	0.0	0.0
Monomer	61.9	100§	88.4	95.0	70.5	50.2	95.5	83.0
Dimer/trimer	27.1	0.0	0.0	0.0	25.1	26.2	2.2	7.8
Pentamer/hexamer	11.0	0.0	0.0	0.0	4.4	23.6	2.3	9.2
			Adsorbed IL-2					
Surface Concentration (μg/cm^2)								
FTIR	0.0	0.05¶	0.31	1.1	0.0	0.05	0.12¶	0.44
Mass balance from solution assay†	0.0	0.12 ± 0.07‡	0.5 ± 0.1	0.92 ± 0.2	0.0	0.08 ± 0.03	0.35 ± 0.1	0.43 ± 0.11

*The Roussel-Uclaf batch records give activities for their bioassay equivalent to 12 ± 6 × 10^5 and 6.0 ± 3.0 × 10^5 units/ml for the 0.1 and 0.05 mg/ml solutions, respectively; errors represent standard deviations of octuplicate assays.
†Concentrations corrected for adsorption in nonflow system; error propagated from standard deviations of the protein assay standardization curve.
‡Samples determined at 4 hr.
§A tail at low retention times signifies the presence of higher molecular weight species; their actual size is indeterminant.
¶Samples determined at 6 hr.

from solution by adsorption to the catheter surface, thereby reducing the total activity. The delivered IL-2 concentration was measured at 2-hr intervals; only the 2-, 10-, and 24-hr measurements are shown in Table 1. At 24 hr, the delivered IL-2 concentration was 20–30% less than that charged to the device, after correction for adsorption to the reservoir. The adsorptive losses are higher on a percentage basis for the lower concentration solution, reflecting the adsorptive capacity of the tubing. Thus, adsorptive losses can only account for a fraction of the observed bioactivity reduction.

For both initial IL-2 concentrations, the adsorptive losses occur rapidly during the first 4 hr. After this point, the delivered concentrations appear to level off. This pseudo-steady state may reflect a shift from kinetic to thermodynamic control of protein adsorption as the competition for adsorption sites stiffens and as adsorbed species optimize their interactions with the surface (23).

Adsorbed IL-2 Concentration Profile. To show that protein was indeed adsorbed to the catheter, we examined the exposed tubing via FTIR spectroscopy. The concentration of IL-2 adsorbed on the catheter as a function of exposure time, calculated from the FTIR amide II band spectra as well as that obtained from a mass balance from the bicinchoninic acid assay of the solution concentration, is given in Table 1. The results from these techniques are in good agreement, indicating that our spectral processing is conservative. As expected, the surface concentration is higher when the solution concentration is higher. The surface concentrations in both the 0.05 and 0.1 mg/ml solution experiments track upwards, indicating that the adsorptive capacity of the tubing has not yet been reached. Our calculated value for monolayer coverage (5) and the Euclidean area of the tubing imply that there are multiple layers of IL-2 on the surface after 24 hr of exposure, in agreement with the reported behavior of silicone rubber surfaces in similar adsorption studies (24). However, by accounting for the roughness of the tubing surface, we estimate that the actual surface coverage is closer to a single IL-2 layer after 24 hr of exposure.

Adsorbed IL-2 Secondary Structure. Numerous studies have shown that protein–surface interactions can be denaturing, particularly when the surface is hydrophobic (25). Amide I band IR spectra for adsorbed IL-2 and the underlying component bands obtained by our deconvolution procedure are shown as a function of exposure time in Fig. 1; the corresponding secondary structure estimates are listed in Table 2. Native IL-2 in solution is a highly helical protein, as shown by the intense band located at 1657 cm^{-1}; α-helix content comprises almost 63% of the structure. This is in good agreement with published IL-2 structural analyses that indicate a total of 42–65% helix and little or no β-sheet content (16, 26). The band appearing at 1630 cm^{-1} can be assigned to extended loop structures that connect the helical segments of the four-helix bundle.

Upon adsorption, IL-2 molecules lose an important part of their native structure; α-helices and extended loop bands disappear while β-sheet signals appear. After 2 hr of surface exposure, the prominent α-helix signal is replaced by intense β-sheet bands located at 1625, 1633, and 1639 cm^{-1} and a random structure band at 1650 cm^{-1}; at this point, β-sheet and random structures compose ≈50% and 25% of the secondary structure content, respectively. Over time, the patterns of increased β-sheet and random structures persist (≈43% and 13% of the structure at 24 hr, respectively), while there is partial recovery of α-helix (≈20%) and diminution of β-turn (≈12%) bands. Either the sampled surface population relaxes to a more native-like state, or the subsequently deposited IL-2 molecules fail to undergo the initial dramatic secondary structure changes. During this time, the dominant β-sheet band position shifts from 1625 (2 and 6 hr) to 1631 cm^{-1} (24 hr). This high wavenumber β-sheet shift is accompanied by a

Downloaded at Palestinian Territory, occupied on December 20, 2021

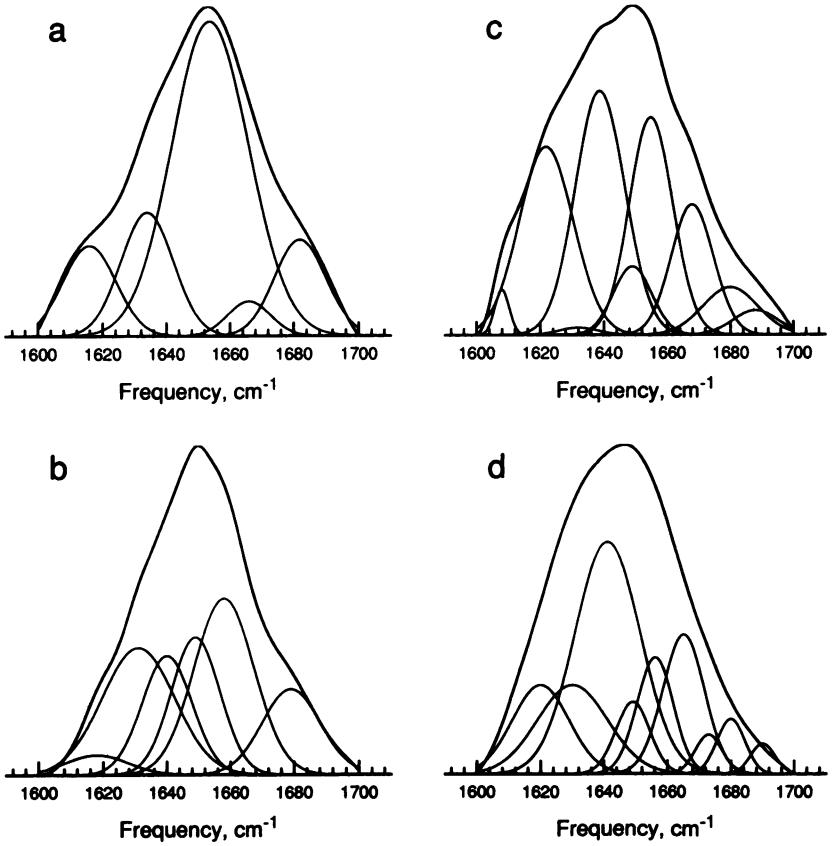

FIG. 1. Deconvoluted and curve-fitted infrared amide I band envelopes of IL-2 (*A*) in solution and adsorbed on the catheter after 2 hr (*B*), 6 hr (*C*), and 24 hr (*D*). The IL-2 concentration charged to the device was 0.1 mg/ml. Spectra are corrected for buffer, silicone rubber tubing, and water vapor contributions where appropriate (5).

similar rearrangement of the β-turns, as their major band shifts from 1667 to 1679 cm^{-1} after 24 hr, indicating stronger hydrogen bonding patterns of the surface-stabilized molecules. Thus, IL-2 is denatured upon adsorption to silicone rubber tubing.

Table 2. Secondary structure of adsorbed and delivered IL-2 as a function of exposure time

	Initial solution	Surface exposure time 2 hr	6 hr	24 hr
Adsorbed IL-2:				
FTIR estimates (structure %)				
α-Helix	63	8	19	28
β-Sheet	0	48	48	42
β-Turns	17	20	21	13
Random	0	25	12	17
Extended	20	0	0	0
Delivered IL-2:				
CD estimates (structure %)*				
α-Helix	65	19	31	39
β-Sheet	10	50	43	38
β-Turns	16	23	17	9
Random	10	11	8	7
Nonflow control:				
CD estimates (structure %)*				
α-Helix	65	54	56	52
β-Sheet	10	20	24	21
β-Turns	16	16	10	13
Random	10	9	10	13

All data correspond to 0.1 mg/ml delivery experiment.
*Standard errors associated with CD estimates were determined to be on the order of ±6% via the use of the SELCON program (9) on a series of native IL-2 solution spectra.

Delivered IL-2 Secondary Structure. To probe the hypothesis that surface-denatured protein may desorb and persist in solution, we analyzed the delivered IL-2 samples via CD spectroscopy. Far-UV CD spectra of the delivered IL-2 as a function of exposure time are shown in Fig. 2; the corresponding secondary structure estimates are given in Table 2. The initial solution sample estimates are in good agreement with the FTIR results. Deconvolution results for the flow system spectra show a rapid ≈75% decrease in α-helix content and an

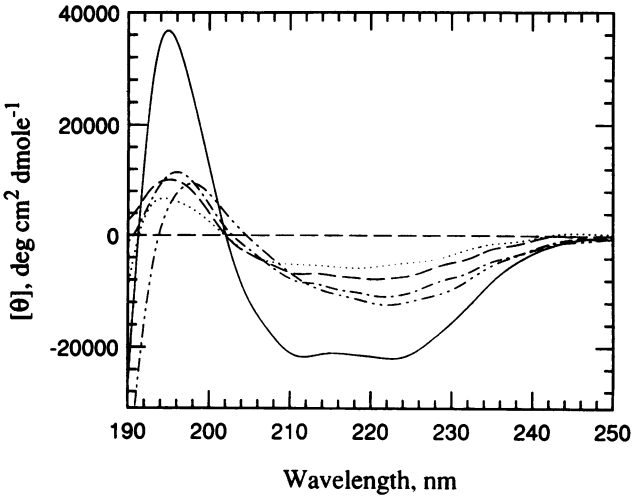

FIG. 2. Far-UV CD spectra of delivered IL-2 as a function of exposure time are shown: native IL-2 in solution (——) and after 2 hr (·····), 6 hr (— —), 12 hr (– ·–), and 24 hr (– · · –) of exposure to the catheter. All spectra refer to 0.1 mg/ml delivery experiments.

Downloaded at Palestinian Territory, occupied on December 20, 2021

increase in β-sheet content relative to the nonflow system over the first 2 hr of delivery. After longer exposure times, the secondary structure contents appear to relax back toward the initial native contents. This apparent partial recovery of helix content likely reflects changing protein populations in solution as time progresses. At all exposure times, there is good agreement between the CD structural estimates for delivered IL-2 and the FTIR structure estimates for adsorbed IL-2. This agreement is particularly striking with respect to the rapid loss and partial recovery of helix content as well as the increase in β-sheet content on surface exposure. These results are consistent with the hypothesis above.

Delivered IL-2 Tertiary Structure. To further probe the conformational status of the delivered protein, fluorescence spectroscopy was employed. Steady-state fluorescence spectra of IL-2 during delivery, which are indicative of the polarity of the environment of the lone Trp residue at position 121, are shown in Fig. 3. The maximum intensity of the initial native IL-2 emission spectrum is located at 328 nm, indicating that Trp^{121} is buried in the interior of the helix bundle (11, 12). For IL-2 denatured in 6 M guanidinium chloride, there is a 30-nm red shift of the emission maximum, indicating that this residue becomes solvent-exposed. Also, a signal intensity comparison of these spectra reveals substantial fluorescence quenching in the native state. This quenching is thought to arise via interaction with the neighboring Cys^{125} residue (11, 12). When the C-terminal helix on which both Trp^{121} and Cys^{125} reside is disrupted, this quenching is reduced; this helix is known to be crucial for biological activity (27). After 2 and 6 hr of surface exposure, the IL-2 samples exhibit a 12- to 15-nm red shift as well as a dequenching, which are intermediate to the native and guanidinium chloride-denatured spectra, indicative of a large population of nonnative molecules in the solution. The static quenching experiments yielded similar results as shown by the Stern–Volmer plots in Fig. 4. In native IL-2, Trp^{121} is buried in the core of the four-helix bundle and is inaccessible to iodide and partially accessible to acrylamide, in good agreement with literature studies on IL-2 (11, 12) and human growth hormone (10). In the guanidinium chloride-denatured state, Trp^{121} becomes fully accessible to both quenchers. The surface-exposed samples (2- and 6-hr) again give results intermediate to the native and guanidinium chloride-denatured states. Trp^{121} has become partially accessible to both quenchers after incubation with the tubing, indicating a swelling or partial unfolding of the delivered IL-2 molecules.

DISCUSSION

To elucidate the role of protein–surface interactions in a medical-grade silicone standard central venous catheter, common to virtually all implantable and portable delivery systems, we examined the biological activity and structural stability of IL-2 during delivery at 37°C. In agreement with previously published clinical studies that ascribed the bioactivity losses of IL-2 during continuous infusion to deposition on the polyethylene catheter tubing (6), we found order of magnitude bioactivity losses resulting after exposure of the protein solution to silicone rubber catheter tubing. Losses due to deposition were significant but small; losses due to incubation at elevated temperature, shear-induced denaturation, and surface-mediated aggregation were insignificant. The majority of these losses were attributed to transient, denaturing interactions between IL-2 and the surface of the catheter. The similarities between the secondary structure analyses of adsorbed IL-2 by FTIR spectroscopy and delivered IL-2 by CD spectroscopy, both in extent of perturbation of the native helical structure and in temporal pattern, are consistent with this interpretation. The Trp^{121} emission spectra and static quenching results for delivered IL-2 provide further insight into the nature of the surface-induced perturbation and the observed loss of activity: the catheter surface induces a transition to a state with expanded hydrophobic core (10) accompanied by alterations in helix D, which is critical for biological activity (27). The surface catalyzes structural changes that are not readily reversed upon desorption.

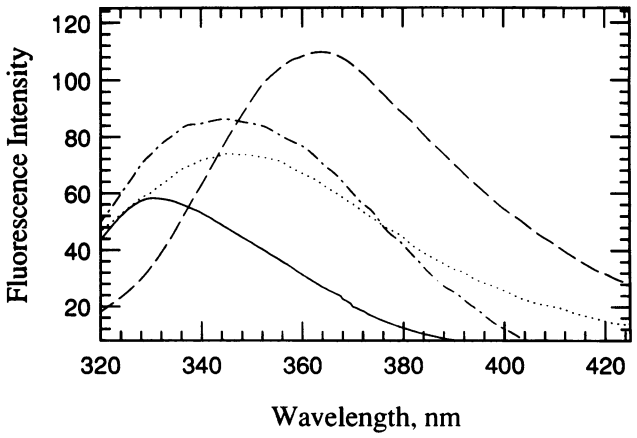

FIG. 3. Tryptophan emission spectra of delivered IL-2 are shown: native IL-2 in solution (——) and after 2 hr (·····) and 6 hr (–·–) of exposure to the catheter, and denatured IL-2 in 6 M guanidinium chloride (— —). All spectra refer to 0.1 mg/ml delivery experiments.

Protein denaturation upon surface interaction is a well-documented phenomenon (28–32). Kondo *et al.* (29) have indicated that a relationship exists between the extent of surface-induced conformational changes and the value of the adiabatic compressibility, β_s, of the protein. The value of β_s for IL-2, as calculated from its partial specific volume (32), is 9.77×10^{12} $cm^2 dyne^{-1}$ (1 dyne = 10 μN). This is close to the value reported for bovine serum albumin, which is known to undergo dramatic conformational changes upon surface exposure (28, 29). It has also been shown by Gavish *et al.* (33) and Gekko *et al.* (32) that α-helices, in contrast to β-sheets, form dynamic domains of the protein structure and are responsible for volume and energetic fluctuations of proteins in the solution state; this may predispose helical proteins such as IL-2 to alterations upon adsorption. Further, in lattice-based simulations of homopolymer chains adsorbing to surfaces, the chains were observed to "dock" initially and then flatten out, undergoing conformational changes as the polymer–surface contacts are maximized (34). The same studies also indicated that certain types of organized secondary structures become prevalent as a surface is approached. These altered, surface-adapted species may desorb due to unfavorable lateral interactions on the surface or to the attainment of an unstable, high-energy intermediate state (35, 36).

Structure analyses of adsorbed species indicate that the extended loop structures of IL-2 disappear upon adsorption, tempting speculation as to the mechanism by which the protein and surface interact. The loops are on the exterior of IL-2 and are rich in hydrophobic residues and are therefore likely to be the part of the molecule that is first presented to the surface. Chou and Scheraga (5) have proposed that the loop–helix interactions are crucial to the structural integrity of four-helix bundle proteins like IL-2. We hypothesize that once these segments are involved in surface interactions, their stabilizing effect on the four-helix bundle is dissipated. As a consequence, the helices of the molecule are able to engage the surface, initiating a surface-contact optimization process, resulting in further deviations from the native structure.

IL-2 is one of a number of pharmaceutical proteins that are currently under clinical investigation for intermittent and/or continuous infusion, pump-based delivery strategies. However, with the currently available devices and catheters, such treatment programs do not guarantee complete or even predictable delivery. This is of particular concern when the dose-response relationship is highly uncertain.

Downloaded at Palestinian Territory, occupied on December 20, 2021

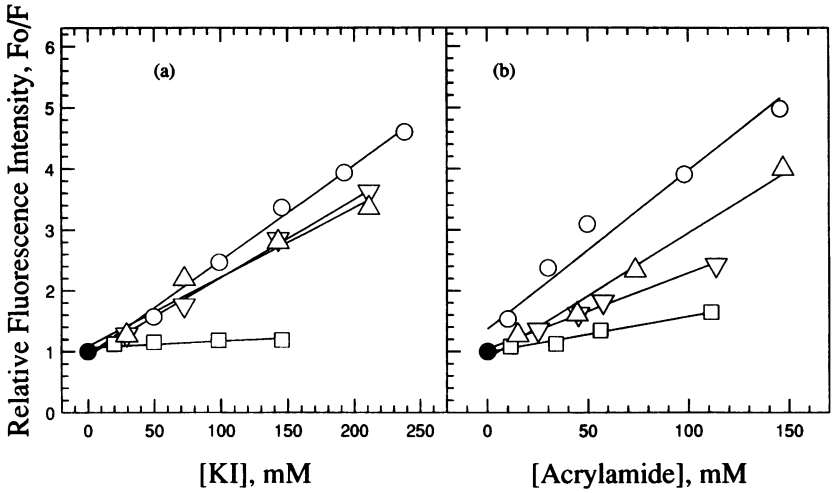

FIG. 4. Stern–Volmer plots of IL-2 static fluorescence quenching with (*A*) iodide and (*B*) acrylamide as quenchers. Symbols used are as follows: □, native IL-2 in solution; ▽ and △, after 2 and 6 hr of exposure to the catheter, respectively; and ○, denatured IL-2 in 6 M guanidinium chloride. Lines represent linear fits to the experimental data. All data refer to 0.1 mg/ml delivery experiments.

We wish to thank Dr. Robert MacColl of the Biochemistry Core Facility, New York State Health Department, for providing access to CD and fluorescence spectrometers. We would also like to thank Medtronic and Disetronic Medical Systems for providing us with the catheters and pumps, respectively.

1. Andrade, J. D. & Hlady, V. (1986) *Adv. Polym. Sci.* **79,** 1–63.
2. Sluzky, V., Klibanov, A. M. & Langer, R. (1992) *Biotechnol. Bioeng.* **40,** 895–903.
3. Sefton, M. V. (1982) in *Biomaterials: Interfacial Phenomena and Applications*, eds. Cooper, S. L. & Peppas, N. A. (American Chemical Society, Washington, DC), pp. 511–522.
4. Visor, G. C., Tsa, K. P., Duffy, J., Miller, M. D., Calderwood, T. & Knepp, V. M. (1990) *J. Parenter. Sci. Technol.* **44,** 130–137.
5. Chou, K.-C., Maggiora, G. M. & Scheraga, H. A. (1992) *Proc. Natl. Acad. Sci. USA* **89,** 7513–7519.
6. Vlasveld, L. T., Beijnen, J. H., Sein, J. J., Rankin, E. M., Melief, C. J. M. & Hekman A. (1993) *Eur. J. Cancer* **29A,** 1979–1981.
7. Sluzky, V., Tamada, J. A., Klibanov, A. M. & Langer, R. (1991) *Proc. Natl. Acad. Sci. USA* **88,** 9377–9381.
8. Tzannis, S. T., Hrushesky, J. M., Wood, P. & Przybycien, T. M. (1994) in *Biomaterials for Cell and Drug Delivery*, eds. Mikos A. G., Murphy, R. M., Bernstein, H. & Peppas, N. A. (Materials Research Society, Pittsburgh), Vol. 331, 227–232.
9. Sreerama, N. & Woody, R. W. (1993) *Anal. Biochem.* **209,** 32–44.
10. Havel, H. A., Kauffman, E. W. & Elzinga, P. A. (1988) *Biochim. Biophys. Acta* **955,** 154–163.
11. Weir, M. P., Chaplin, Wallace, D. M., Dykes, C. W. & Hobden, A. N. (1988) *Biochemistry* **27,** 6883–6892.
12. Dryde, D. & Weir, M. P. (1991) *Biochim. Biophys. Acta* **1078,** 94–100.
13. Lehrer, S. S. & Leavis, P. C. (1978) *Methods Enzymol.* **49,** 222–237.
14. Eftnik, M. R. & Ghiron, C. A. (1981) *Anal. Biochem.* **114,** 199–227.
15. Thomas, C. R., Nienow, A. W. & Dunnill, P. (1979) *Biotechnol. Bioeng.* **21,** 2263–2278.
16. Cohen, F. E., Kosen, P. A., Kuntz, I. D., Epstein, L. B., Ciardelli, T. L. & Smith, K. A. (1986) *Science* **234,** 349–352.
17. Hora, M. S., Rana, R. K., Wilcox, C. L., Katre, N. V., Hirtzer, P., Wolfe, S. N. & Thomson, J. W. (1991) *Dev. Biol. Standard.* **74,** 295–306.
18. Kunitani, M., Hirtzer, P., Johnson, D., Holenbeck, R., Bausman, A. & Koths, K. (1986) *J. Chromatogr.* **359,** 391–407.
19. Browning, J. L., Mattaliano, R. J., Chow, E. P., Liang, S.-M., Allet, B., Rosa, J. & Smart, J. E. (1986) *Anal. Biochem.* **155,** 123–128.
20. Manning, M. C., Patel, K. & Borchardt, R. T. (1989) *Pharm Res.* **6,** 903–917.
21. Arakawa, T., Boone, T., Davis, J. M. & Kenney, W. C. (1986) *Biochemistry* **25,** 8274–8277.
22. Geigert, J., Solli, N., Woehleke, P. & Vemuri, S. (1993) in *Stability and Characterization of Protein and Peptide Drugs: case histories*, eds. Wang, Y. J. & Pearlman, R. (Plenum, New York), pp. 249–262.
23. Soderquist, M. E. & Walton, A. G. (1980) *J. Colloid Interface Sci.* **75,** 386–397.
24. Lok, B. K., Cheng, Y.-L. & Robertson, C. R. (1983) *J. Colloid Interface Sci.* **91,** 104–116.
25. Lu, D. R. & Park, K. (1991) *J. Colloid Interface Sci.* **144,** 271–281.
26. Brandhuber, B. J., Boone, T., Kenney, W. C. & McKay, D. B. (1987) *Science* **248,** 1707–1709.
27. Landgraf, B., Cohen, F. E., Smith, K. A., Gadski, R. & Ciardelli, T. L. (1989) *J. Biol. Chem.* **264,** 816–822.
28. Norde, W. & Favier, J. P. (1992) *Colloids Surf.* **64,** 87–93.
29. Kondo, A., Oku, S. & Higashitani, K. (1991) *J. Colloid Interface Sci.* **143,** 214–221.
30. Kondo, A., Oku, S. & Higashitani, K. (1991) *Biotechnol. Bioeng.* **37,** 537–543.
31. Kondo, A., Murakami, F., Kawagoe, M. & Higashitani, K. (1993) *Appl. Microbiol. Biotechnol.* **39,** 726–731.
32. Gekko, K. & Hasegawa, Y. (1986) *Biochemistry* **25,** 6563–6571.
33. Gavish, B., Gratton, E. & Hardy, C. J. (1983) *Proc. Natl. Acad. Sci. USA* **80,** 750–754.
34. Chan, H. S., Wattenbarger, M. R., Evans, D. F., Bloomfield, V. A. & Dill, K. A. (1991) *J. Chem. Phys.* **94,** 8542–8557.
35. Norde, W., MacRitchie, F., Nowicka, G. & Lyklema J. (1986) *J. Colloid Interface Sci.* **112,** 447–456.
36. Soderquist, M. E. & Walton, A. G. (1980) *J. Colloid Interface Sci.* **75,** 386–397.

Downloaded at Palestinian Territory, occupied on December 20, 2021